Exchange-coupled pairs of Yb^{3+} ions in SrF_2

M. Velter-Stefănescu and S. V. Nistor
Central Institute of Physics, P.O. Box MG-6, Magurele, R-76900 Bucharest, Romania

V. V. Grecu
Department of Physics, University of Bucharest, P.O. Box MG-11, Magurele, R-76900 Bucharest, Romania
(Received 11 December 1985)

Detailed investigations of the spin-lattice relaxation of single Yb^{3+} ions at trigonal sites in SrF_2 are reported. The measurements were performed in the 2–12 K temperature range, in the X band, by using a pulse-sequence saturation method and compared with earlier Q-band measurements. At $T \geq 7.5$ K the relaxation is described at both frequencies by an Orbach process. At lower temperatures ($2 \leq T \leq 6$ K), T_1 exhibits a departure from a linear temperature dependence, unexpected shorter values, and lack of anisotropy. This is interpreted by considering cross relaxation with fast relaxing pairs of exchange-coupled Yb^{3+} ions with the same trigonal symmetry and Zeeman splittings. The spin-lattice relaxation of pairs is governed by an Orbach process which involves transitions between the $S'=1$ ground and $S'=0$ excited states, separated by $J=-12.5$ K. Consequently, the low-temperature ($2 \leq T \leq 12$ K) relaxation of single Yb^{3+} ions is described by

$$T_1^{-1} = \frac{142.2}{\exp(12.5/T)-1} + 7.731 B^5 \coth\left(\frac{h\nu}{2kT}\right) + 0.197\times 10^9 \exp\left(-\frac{111.67}{T}\right) .$$

The analysis of ESR spectra confirms the presence of such weakly exchange-coupled Yb^{3+} pairs with $J<0$, representing about 1% of the total content of Yb^{3+} ions.

I. INTRODUCTION

It is now a well-known fact that trivalent rare-earth ions (R^{3+}) in alkaline-earth fluorides substitute for bivalent cations, the charge compensation occurring by interstitial F^- ions, substitutional O^{2-} and H^- ions and cation vacancies.[1] Consequently, ESR spectra of R^{3+}-doped alkaline-earth fluorides usually reveal, besides cubic R^{3+} centers with remote charge compensation, one or more noncubic R^{3+} centers exhibiting tetragonal symmetry along ⟨100⟩, or trigonal symmetry along ⟨111⟩, consisting of a R^{3+} ion with charge compensators in the near neighborhood.

Until now Yb^{3+} in SrF_2 has been identified either in cubic sites or in trigonal sites, charge compensated either by interstitial F^- or substitutional O^{2-}.[2–5] Previous ESR studies[3,6] on certain SrF_2 single crystals doped with Yb^{3+}, obtained from the same source, have shown that in such crystals all Yb^{3+} ions occur as trigonal centers. It was inferred from superhyperfine structure analysis,[6] as well as from discrete saturation measurements,[7] that the noncubic crystal field was due to the presence of a charge compensating F^- ion in the nearest interstitial position along a ⟨111⟩ direction. This structure (Fig. 1) is known as the T_4 type of center.[1]

Such crystals, with all Yb^{3+} ions in the same crystal-field configuration and free of sizable amounts of other paramagnetic impurities, represent an excellent crystalline system to study the spin-lattice relaxation (SLR) of paramagnetic rare-earth ions.

We have presented in a short paper[8] the results obtained from SLR measurements in the 35-GHz microwave frequency band, by using a pulse-sequence saturation method.[9] The experimental results have shown a dominant direct-process to occur below 4.2 K,

$$T_{1D}^{-1} = 5.88 \coth\left(\frac{h\nu}{2kT}\right) , \quad (1)$$

and an obvious angular dependence, in agreement with the Van Vleck–Kroning mechanism.[10,11] At higher temperatures the experimental data were interpreted by considering an Orbach process

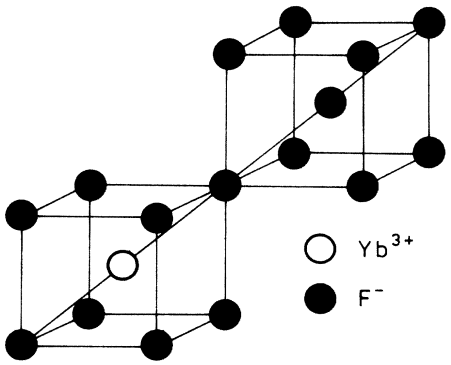

FIG. 1. Structural model of the trigonal T_4 center in alkali earth fluorides.

$$T_{10}^{-1}=0.197\times 10^{9}\exp(-111.67/T)\ . \tag{2}$$

According to the theory[12–14] a strong magnetic-field dependence ($T_{1D}^{-1}\sim B^4$) of the direct-process relaxation time should be observed.

We carried out, on samples from the same single crystal, SLR time (T_1) measurements in the X band (9 GHz). In a most disturbing way, we found in the 2–6 K temperature range a departure from the linear temperature dependence of T_1^{-1}, unexpected short values of T_1 (about 2 orders of magnitude smaller) compared to the values measured in the Q band, as well as an almost complete absence of relaxation-time anisotropy.

We explain all these results by considering the presence of a cross-relaxation mechanism with some fast-relaxing centers, cross relaxation which has been observed directly with our experimental setup. It is shown that the fast-relaxing centers are pairs of exchange-coupled Yb^{3+} ions, with the same trigonal symmetry as the single Yb^{3+} ions. The presence of pairs also explains some peculiarities observed in the low temperature dependence of the EPR line shape of single Yb^{3+} ions.

II. EXPERIMENTAL

The pulse-saturation techniques usually employed in the electron spin-lattice relaxation-time measurements are based on a simple procedure: A high power microwave pulse saturates the spin system, and the relaxation time T_1 is obtained from the recovery curve to its thermal equilibrium state, obtained by means of a very low monitoring power microwave field H_1. Due to the very low monitoring power ($10^{-5}-10^{-9}$ W) usually employed, the desired sensitivity ($\sim 10^{16}$ spins) is generally obtained only with superheterodyne detection.[12–14]

The difficulties of detection at low H_1 can be overcome by applying an $A+nB$ pulse sequence. According to this method[9] a pulse A of length t_A saturates the spins (Fig. 2) and the far shorter equidistant pulses nB of length t_1 monitor the magnetization recovery toward the thermal equilibrium value.

It can be shown[9] that in the presence of inspection pulses the relaxation process still preserves its exponential behavior, the time constant being

$$T_1^{*}=\frac{t_2/t_1+1}{T_1/\tau+t_2/t_1}T_1\ . \tag{3}$$

From the above relation it results that the saturation effects can be neglected as long as

$$t_2/t_1\gg T/\tau \text{ and } t_1\ll t_2 \tag{4}$$

(when the pulses nB are equal in amplitude to the pulses A).

Here t_2 is the time between the inspection pulses B and

$$\tau=(T_1^{-1}+W)^{-1} \tag{5}$$

is the decay time constant of the magnetization during the microwave pulse. W is the probability of the stimulated transition, which is proportional to the microwave power P.

Therefore, for a given microwave power, one determines the value of τ by selecting the ratio t_2/t_1 according to (4). The relaxation process will not be influenced, and the envelope of the inspection pulses yields T_1 (Fig. 3).

In practice, besides considering (4), t_1, t_2, and τ must be chosen in such a way that the relaxation curve is observed with enough inspection pulses. Based on this principle we have built an X band ESR spectrometer-relaxometer which has been used in the present studies. The block diagram is shown in Fig. 4. A 1-W reflex klystron is used as a main microwave power source. The klystron is frequency stabilized to a reference tunable high Q resonance cavity. A homemade pin-diode microwave switch, with an off/on ratio of 60 to 70 dB in the 9–9.5 GHz range, is used to provide the saturating and inspection pulses. The microwave switch is activated from a pulse programmer which gives the $A+nB$ pulse sequence. The pulsed microwave power is connected through a circulator to the sample cavity and thence to a crystal detector. The output of a detector equipped with a Silvania 1N23E diode is amplified by a threshold wide-band amplifier and fed into a storage oscilloscope (Tektronix 5403).

The sample cavity,[15] with an unloaded $Q\sim 9000$, resonates in the TE_{011} mode and is provided with an adjustable coupling to the waveguide. The chief advantage of this cavity is the possibility it offers to change specimens, or to alter the specimen orientation in the cavity, even in the presence of liquid helium. The cavity is provided with a heater and measuring thermometers coupled to an Artronix 5301 E temperature controller, to allow measurements in the variable temperature regime to be performed.

The instrument can be operated as a cw induction spectrometer with homodyne detection too. In such a mode of operation the microwave detector is biased through an

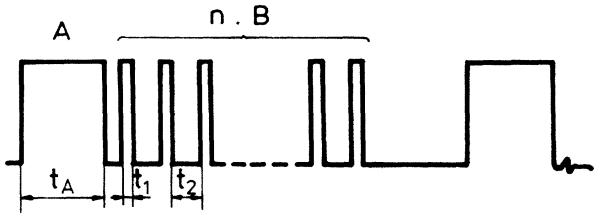

FIG. 2. Pulse sequence for measuring the spin-lattice relaxation time T_1 with high accuracy.

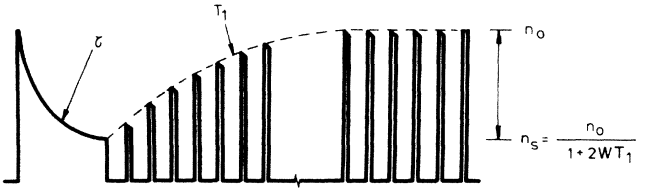

FIG. 3. Typical recovery curve in a relaxation measurement.

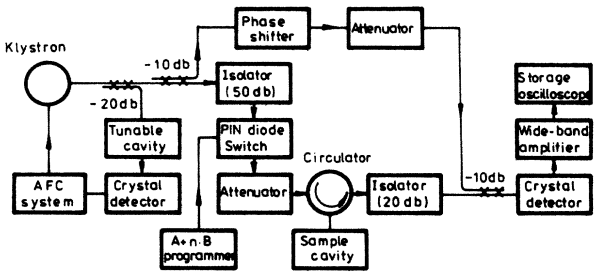

FIG. 4. The block diagram of the ESR spectrometer-relaxometer used in the present study.

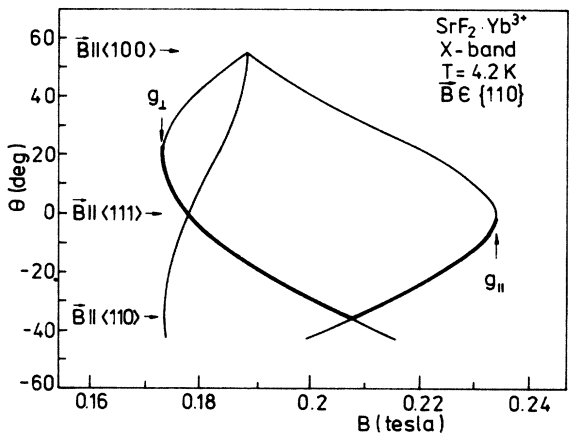

FIG. 5. Angular dependence of the ESR central transition ($I=0$) of Yb^{3+} (T_4) centers in SrF_2 taken with the magnetic field rotated in a (110) plane. The continuous line indicates the ESR transition on which the angular dependence of the spin-lattice relaxation time at 4.2 K was measured.

auxiliary reference arm. Normally the selective amplification and phase-sensitive detection are used in a conventional manner. The 100-kHz field modulation is applied through a single loop inside the cavity.

The relaxation curve appears as the envelope of the sequence of pulses B. The time constant τ is estimated from the decay of the magnetization during the pulse A.

During the relaxation-time measurements it is necessary to decrease the microwave power until one obtains a value of τ much longer than t_1, in order to prevent the saturation during the pulses nB. A value of $\tau \simeq 30t_1$ is a reasonable one. The repetition time t_2 is taken in such a way as to obtain enough inspection pulses B during the recovery of the spins system to equilibrium, which should last for about $3T_1$ to get in a good approximation the relaxation curve. The condition (4) is fulfilled when the time constant of the relaxation curve does not change by increasing t_1, or decreasing t_2.

With our experimental setup the minimum value of T_1 to be measured is about 10μsec. This value results from the minimum attainable value of t_2 (~ 0.3 μsec), as determined by the rise and fall times of the microwave pulses and by the cavity's own ringing time ($Q/2\pi\nu \sim 0.2$ μsec). It is possible to decrease the cavity Q, but this would result in a degradation of the signal-to-noise ratio. However, for shorter relaxation times the inspection pulses nB might be omitted since one can operate with larger monitor powers, so that the usual pulse-recovery method can be used, which makes it possible for relaxation times of about 1 μsec to be measured. After our estimation, a limiting sensitivity of about 10^{16} spins has been obtained, similar to the one obtained with the superheterodyne detection,[16] but with a much simpler experimental setup.

The samples used in this work were cleaved from the same larger piece of SrF_2 doped in melt with 0.1 wt. % of YbF_3. The single crystalline ingot was grown from melt, at the Institute for General Physics in Moscow, by the Bridgman technique in graphite crucibles, in a fluorine atmosphere.

III. RESULTS

A. T_4 centers in SrF_2·Yb^{3+}

Under the influence of a trigonal crystal field with C_{3v} symmetry the eightfold degenerate $4f^{13}\,^2F_{7/2}$ ground term of the Yb^{3+} ion splits into four Kramers doublets.[17] Since our research no optical data on any trigonal Yb^{3+} center in SrF_2 are available, so the energy levels and wave functions are not available and consequently no detailed relaxation calculations can be made.

The ESR spectrum obtained by rotating the magnetic field in a (110) plane consists (Fig. 5) of three main lines from the T_4 centers oriented along the four ⟨111⟩ directions (two of which are equivalent for this particular plane) and several weak hfs lines due to Yb^{171} ($I=\frac{1}{2}$, natural abundance 14.27%) and Yb^{173} ($I=\frac{5}{2}$, natural abundance 16.08%) isotopes.

The ESR spectrum is described[3] by the spin-Hamiltonian

$$\mathcal{H}_s = g_{\parallel}\beta B_z S_z + g_{\perp}\beta(B_x S_x + B_y S_y) + A S_z I_z + B(S_x I_x + S_y I_y) \quad (6)$$

with $S=\frac{1}{2}$ and $I=0$, $\frac{1}{2}$, or $\frac{5}{2}$, depending on what nuclear isotope is considered. The spin-Hamiltonian parameters are given in Table I. Additional terms should be considered in (6) to describe the superhyperfine interaction with neighboring fluorine nuclei.[6,7]

It is known[1] that in a cubic crystal field the lowest doublet is

$$\Gamma_7^{\pm} = \pm\frac{\sqrt{7}}{3\sqrt{2}}\,|\pm\tfrac{7}{2}\rangle + \frac{\sqrt{10}}{3\sqrt{2}}\,|\pm\tfrac{1}{2}\rangle \mp \frac{1}{3\sqrt{2}}\,|\mp\tfrac{5}{2}\rangle\,,$$

TABLE I. Parameters of the spin-Hamiltonian for single Yb^{3+} ions (T_4 centers) and trigonal Yb^{3+}-Yb^{3+} pairs in SrF_2.

	Yb^{3+} single ion	Yb^{3+}-Yb^{3+} pair
$g_{\parallel}$	2.813±0.002	2.813 ±0.006
$g_{\perp}$	3.746±0.002	3.746 ±0.006
^{171}A	55.7 ±0.3 mT	
^{171}B	55.5 ±0.3 mT	
^{173}A	15.3 ±0.3 mT	
^{173}B	15.5 ±0.2 mT	
J		−8.7 ±0.7 cm^{-1}
D_e		0.0089±0.0003 cm^{-1}

which yields an isotropic g_{cub} value of 3.429. The g values of the T_4 center in SrF_2 are consistent with a doublet derived from the cubic Γ_7, since $\frac{1}{3}(g_{\parallel}+2g_{\perp}) = 3.468 \simeq g_{cub}$. It also indicates that the other doublets derived from $^2F_{7/2}$ are sufficiently far away to have little effect on the g values. Indeed, our earlier SLR measurements in the Q band[8] have shown that for higher temperatures an Orbach-type of process is predominant, with the excited state situated at $\Delta = 77.6$ cm^{-1} above the ground doublet.

B. Spin-lattice relaxation-time measurements

SLR time measurements performed in the X band, along a $\langle 111 \rangle$ direction ($g_{\parallel}$ orientation), show the magnetization recovery curves, obtained in the 2–6 K temperature interval, to be described by two exponentials with sharply different time constants. The relative weight of the fast exponential is dependent to a great extent on the length of the saturating pulse, which is a strong evidence of cross relaxation. In order to separate the SLR time T_1 from the spin-spin cross-relaxation time T_{21}, the saturating pulse length was varied from 25 μs to 0.5 ms and the relaxation time T_1 was measured in the tail of the recovery curve. For higher temperatures (above 6 K) single exponential recovery curves were observed.

The temperature dependence of T_1 indicates (Fig. 6) the dominant process above 7.5 K to be, as in the Q band, an Orbach-type process,

$$T_{10}^{-1} = 0.197 \times 10^9 \exp(-111.67/T) . \quad (7)$$

In the lower temperature range (below 6 K), where the direct process is dominant, a departure from a T_1^{-1} temperature dependence was observed (Fig. 7).

Another discrepancy with our earlier data[8] results from comparing the angular dependences of the SLR time for the direct process. When the magnetic field is rotated in a (110) plane, away from a $\langle 111 \rangle$ direction, no essential changes in the magnitude of T_1 were observed for the X-band measurements, in contradiction to the earlier data taken in the Q band, where a clear angular dependence was obtained (Fig. 8).

These puzzling results can be understood if one considers the presence of an additional mechanism contributing to the relaxation of Yb^{3+} ions. Indeed, the presence in the low temperature range, in the X-band measurements, of a fast-relaxing component is a strong argument that cross relaxation with certain fast-relaxing centers should be taken into consideration.

A large variety of such fast-relaxing centers could exist: other paramagnetic impurities, Yb^{3+} ions at sites with different symmetries, or clusters of two or more Yb^{3+} ions.[14,17] In general their effect should manifest only in magnetic fields of certain strength and direction. In our case T_{21} changes in a very limited range over all angles (from about 35–50 μsec) and T_1 exhibits an isotropic

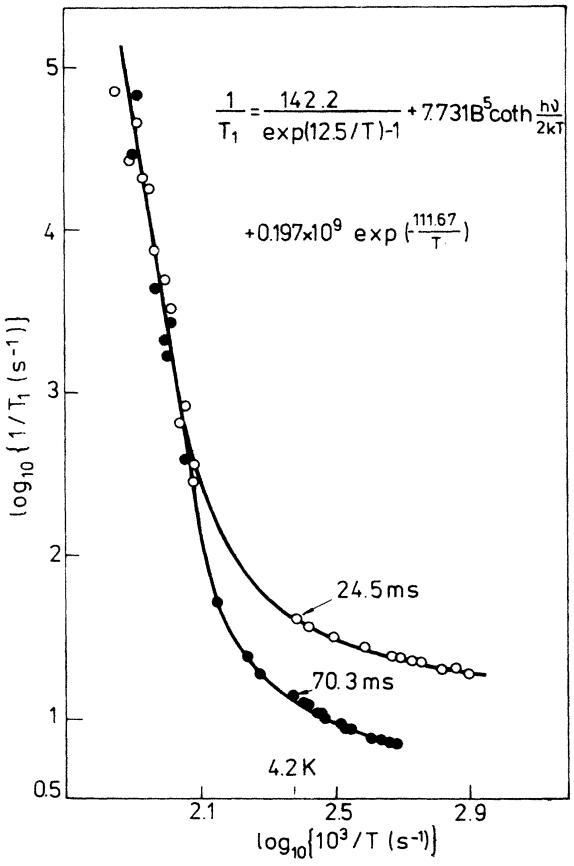

FIG. 6. Temperature dependence of the relaxation rate for Yb^{3+} (T_4) centers in SrF_2 with the magnetic field along the local C_3 axis ($g_{\parallel}$ line). Open circles: Q-band data (Ref. 8); solid circles: X-band data.

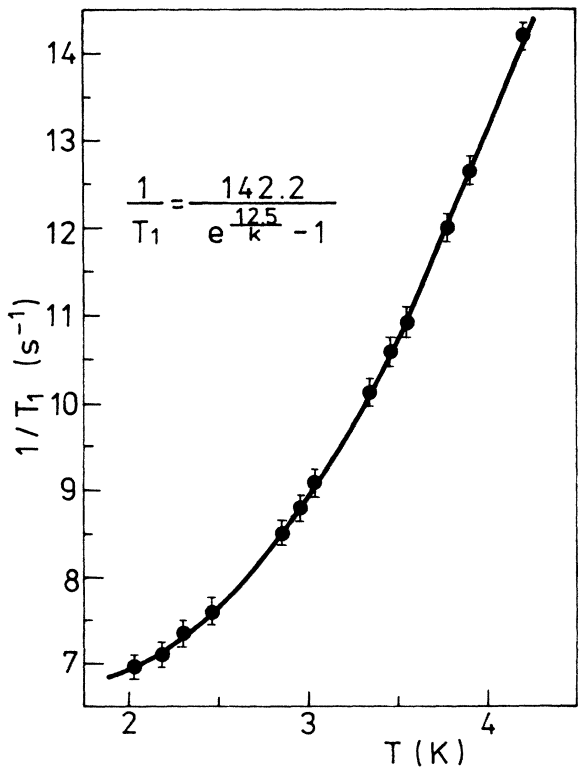

FIG. 7. Low-temperature dependence (2 K $\leq T \leq$ 6 K) of the relaxation rate for the Yb^{3+} (T_4) centers in SrF_2 ($g_{\parallel}$ line) in the X band.

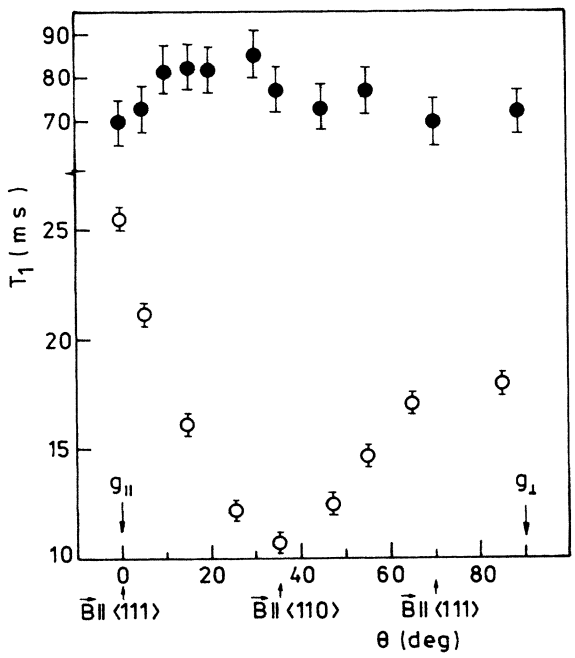

FIG. 8. Angular dependence of the observed relaxation time T_1 as a function of the angle between the magnetic field and the local C_3 axis of the center. Open circles: Q-band data (Ref. 8); solid circles: X-band data: $T=4.2$ K.

character. It means that the fast-relaxing centers have similar angular dependence and Zeeman splittings like the isolated Yb^{3+} ions. As will be further argued, such conditions could be fulfilled only by centers consisting of pairs of Yb^{3+} ions, magnetically coupled along a ⟨111⟩ direction.

In choosing pairs as fast-relaxing centers, besides the absence of known paramagnetic ions with angular dependence and Zeeman splittings in SrF_2 like the trigonal (T_4) Yb^{3+} center,[17] we were supported by the known fact[18] that exchange-coupled pairs can relax much faster than single ions. Indeed, due to the greater number of energy levels present in the pairs, there are more possibilities for the transfer of energy to the lattice. Moreover, the exchange interactions, which depend very strongly on the distance between the coupled ions, make relaxation mechanisms based on the modulation of exchange interactions very effective. Also, changes in the local symmetry can make the Van Vleck mechanism for pairs faster than for the isolated ions.

The simplest structural model of such a pair center is presented in Fig. 9. It has a Yb^{3+}-F^--F_i^--F^--Yb^{3+} configuration along its symmetry axis, the central interstitial F^- ion partly compensating the excess charge of the Yb^{3+} ions.

As will be shown in the next paragraph we have been able to identify ESR signals attributed to such pairs. Before that, we shall explain how the relaxation of Yb^{3+} ions, observed at lower temperatures, can be understood by considering an additional relaxation mechanism with pairs.

Accepting the presence of cross relaxation via pairs, the low-temperature SLR rate T_1^{-1} of isolated Yb^{3+} ions becomes a sum of the intrinsic direct process rate T_{1D}^{-1} and an additional relaxation rate T_{1A}^{-1} due to the spin-lattice relaxation through pairs:

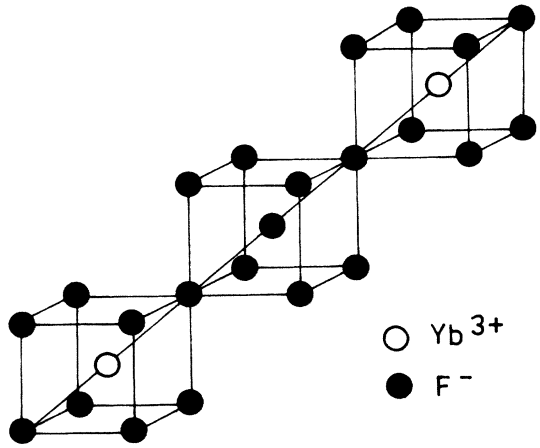

FIG. 9. Proposed structural model of the fast-relaxing exchange-coupled trigonal Yb^{3+} pair in SrF_2.

$$T_1^{-1}=T_{1D}^{-1}+T_{1A}^{-1}\ . \tag{8}$$

The temperature and angular dependence of the relaxation rate at low temperatures indicates the intrinsic direct process is dominant in the Q band and the additional relaxation process is dominant in the X band, which means

$$T_{1D}^{-1}\gg T_{1A}^{-1}\ \ (Q\text{ band})\ , \tag{9a}$$

$$T_{1A}^{-1}\gg T_{1D}^{-1}\ \ (X\text{ band})\ . \tag{9b}$$

These inequalities are also a consequence of the strong magnetic-field dependence ($T_{1D}^{-1}\sim B^4$) of the intrinsic direct process.[10] Moreover, comparing numerical values of T_1, in both microwave bands, at the same temperature (70.3 ms in the X band and 24.5 ms in the Q band, at 4.2 K), one concludes that the relaxation through pairs is almost magnetic-field independent. Indeed any B^m dependence of T_{1A}^{-1}, where m is an integer, would yield a much smaller value of T_1 in the X band.

In such circumstances we shall consider for the pair relaxation on Orbach-type of process, with the relaxation rate given by

$$T_{1P}=\frac{A}{\exp(|J|/kT)-1}\ , \tag{10}$$

where $|J|$ is the isotropic exchange integral and $A\sim|J|^3$ is a temperature-independent factor.[18]

We have considered an Orbach process for the following reasons: Firstly, it can be more rapid than a simple direct process, as it involves phonons of energy $|J|\gg\delta$ (δ is the Zeeman splitting) which arise from a much densely populated part of the phonon spectrum.[19] Thus, condition (9b) is satisfied. Secondly, the Orbach process is magnetic-field independent, which would explain the preponderance of the intrinsic direct process by going from lower (X band) to higher (Q band) magnetic fields.

In the limit of a strong cross relaxation, T_{1A} is related to the "pairs" relaxation-time T_{1P} by:

$$T_{1A}^{-1}\simeq\frac{N_p}{N_s}T_{1P}^{-1}\ , \tag{11}$$

where N_p and N_s are, respectively, the populations of the pairs and single-ion levels.[20] From (10) and (11) one obtains:

$$T_{1A}^{-1} \simeq \frac{N_p}{N_s} A[\exp(|J|/kT)-1]^{-1} . \quad (12)$$

As shown in Fig. 7 the temperature dependence of the experimental relaxation rate in the X band is indeed well fitted by Eq. (12) with $|J| = 12.5$ K, i.e.,

$$T_{1A}^{-1} = 142.2[\exp(12.5/T)-1]^{-1} , \quad (13)$$

which confirms the validity of our assumptions.

C. ESR spectra of Yb^{3+} pairs

From the analysis of SLR data of isolated Yb^{3+} ions (T_4 centers) it has been inferred that a certain amount of Yb^{3+} pairs should be present too. Pairing of Yb^{3+} ions with spin $S = \frac{1}{2}$ generates centers with spin $S'=0$ and 1, which can be described[18] by the spin Hamiltonian

$$\mathcal{H}_P = W_{s'} + \beta \mathbf{B} \hat{g} \mathbf{S}' + D_{s'}[(S_z')^2 - \tfrac{1}{3}S'(S'+1)] , \quad (14)$$

where

$$W_{s'} = \frac{J}{2}[S'(S'+1) - S_i(S_i+1) - S_j(S_j+1)] . \quad (15)$$

J is the isotropic exchange integral and $D_{s'}$ represents the anisotropic interaction with axial symmetry consisting of two terms, the dipolar term D_d and the pseudodipolar exchange term D_E:

$$D_{s'} = \tfrac{3}{2}D_e = \tfrac{3}{2}(D_d + D_E) . \quad (16)$$

The associated energy-levels diagram consists of a singlet state ($S'=0$) separated from the triplet state ($S'=1$) by J, the relative positions being determined by the sign of J. For $|J| \gg g\beta B$ the ESR transitions take place inside the triplet. Besides the two "allowed" transitions ($|\Delta m_{s'}| = 1$: $m_{s'} = \pm 1 \leftrightarrow m_{s'} = 0$) separated by

$$\Delta H_\alpha = D_{s'}\left[3\frac{g_{\parallel}^2}{g^2}\cos^2\theta - 1\right] , \quad (17)$$

where θ is the angle between the "intermetallic" Yb^{3+}-Yb^{3+} vector and the external field, the mixing of the pair wave functions by the $D_{s'}$ term partly allows the "forbidden" transition ($|\Delta m_{s'}| = 2$: $m_{s'} = -1 \leftrightarrow m_{s'} = 1$). The forbidden transition should be visible at half the average magnetic field of the "allowed" transitions.

In order to check the validity of these conclusions, as well as to determine the sign of J, we have performed a careful analysis of the ESR spectra, in the best conditions of sensitivity ($T = 4.2$ K, X band, microwave power ~ 1 μW).

Due to the relatively small concentration of Yb^{3+} pairs and the superposition of the strong ESR lines from single Yb^{3+} ions, resulting from similar symmetry and Zeeman splittings, it has been possible to identify ESR lines attributed to Yb^{3+} pairs only for certain orientations of the magnetic field.

Thus, with the magnetic field oriented along a ⟨111⟩ direction, one can see (Fig. 10) superimposed on the ESR line of the single Yb^{3+} ions (the $g_{\parallel}$ line) two weak lines attributed to the $|\Delta m_{s'}| = 1$ transitions of the Yb^{3+} pairs, with the symmetry axis along the same ⟨111⟩ direction. From the separation of these two allowed transitions one obtains $D_{s'} = 13.4 \times 10^{-4}$ cm^{-1}. For the same orientation of the magnetic field the forbidden transitions of the pairs cannot be distinguished from the strong ESR lines of the single Yb^{3+} ions oriented along the other three ⟨111⟩ axes.

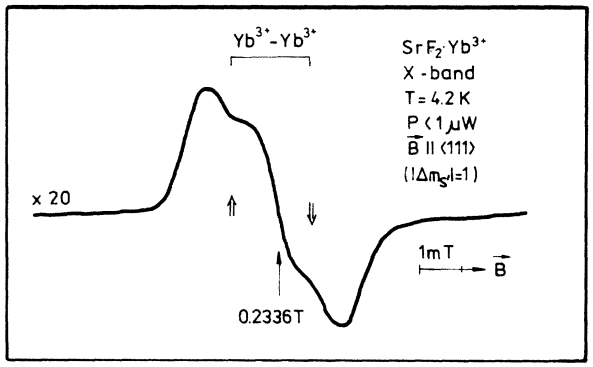

FIG. 10. ESR line attributed to the $|\Delta m_{s'}| = 1$ transitions of the Yb^{3+} pair-centers, superimposed on the $g_{\parallel}$ line of single Yb^{3+} ions.

The maximum separation of 2.05 mT between the allowed transitions of Yb^{3+} pairs, attained with the magnetic field along a pair axis, is of the same magnitude as the half-width of the single Yb^{3+} ions lines. Consequently, the overlap of the pairs and single-ion lines is always present, which assures the effectiveness of cross relaxation for all orientations.

By rotating the magnetic field with an angle θ, away from ⟨111⟩, the separation of the allowed transitions changes like $3\cos^2\theta - 1$. Practically, it means that for $\theta > 15°$ the two lines overlap and become undistinguishable from the ESR line of single Yb^{3+} ions on which they are superimposed, as has been experimentally checked.

With $\mathbf{B} \| \langle 100 \rangle$, all trigonal centers are magnetically equivalent, the ESR spectrum is simplified, and the central ($I=0$) transition of single Yb^{3+} ions, as well as the allowed transitions of Yb^{3+} pairs, are centered at $B = 188.2$ mT. As expected, the forbidden transition of Yb^{3+} pairs is visible at half-field (94.1 mT) (Fig. 11).

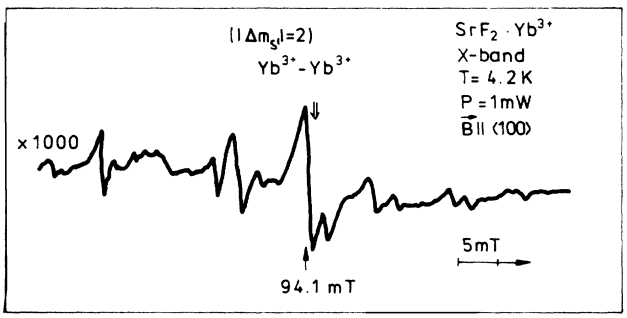

FIG. 11. ESR line attributed to the $|\Delta m_{s'}| = 2$ transitions of the Yb^{3+} pair centers for $\mathbf{B} \| \langle 100 \rangle$. The weaker lines belong to various hyperfine transitions of the ytterbium isotopes with $I \neq 0$.

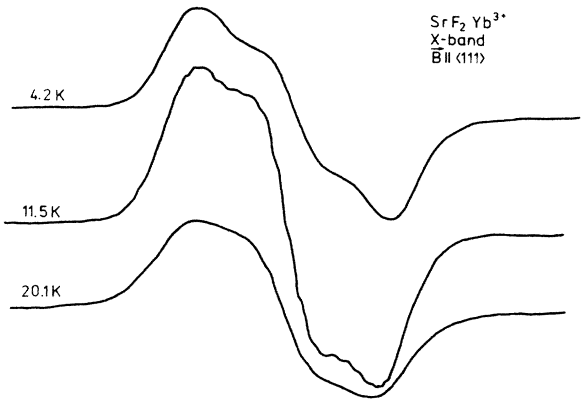

FIG. 12. Shape of the ESR line attributed to the superposition of the $g_{||}$ transition from single Yb^{3+} ions and the "allowed" transitions of Yb^{3+} pair centers with the same orientation, at various temperatures. At certain temperatures ($T\sim 11$ K) the superhyperfine structure due to the interaction between the unpaired f electrons of single Yb^{3+} ions and the neighboring F^{19} nuclei is partly resolved.

The fact that the allowed transitions of the Yb^{3+} pairs are superimposed on the ESR transitions of isolated Yb^{3+} ions, exhibiting similar angular dependences, arouses some suspicions concerning their different origin; it would seem possible that we are dealing with a partly resolved superhyperfine (shf) structure due to the magnetic interaction of the unpaired electron with the neighboring fluorine nuclei. However, the different temperature dependence of the line shape for the parallel orientation, in the 4.2–20 K temperature interval (Fig. 12), proves that we are indeed dealing with a superposition of ESR lines arising from two types of paramagnetic centers.

The concentration of Yb^{3+} pairs, estimated from the relative intensity of the allowed transitions for $\mathbf{B}||\langle 111\rangle$ is about 1% of the concentration of single Yb^{3+} ions. The temperature variation of the ESR line intensity of Yb^{3+} pairs indicates that $J<0$, i.e., the triplet state is indeed the lowest.

IV. DISCUSSION

We have measured in the X band the spin-lattice relaxation time of single trigonal Yb^{3+} ions (T_4 centers) in SrF_2, and compared our new results with earlier data obtained in the Q band. To understand the observed differences we had to accept the presence of a fast cross-relaxation process with other paramagnetic entities, exhibiting the same symmetry and Zeeman splittings. We have shown that such entities are Yb^{3+} pairs oriented along a $\langle 111\rangle$ direction, which relax to the lattice, in the low temperature region, through an Orbach process (10).

The Orbach-type process involves transitions between the $S'=0$ excited state of the pairs and the $S'=1$ ground state. Such transitions can be induced only by perturbations resulting from antisymmetric modes, in which the ions vibrate out of phase.[18] Since the amplitudes of the antisymmetric modes are about a factor $\alpha=\pi r_{ij}/\lambda$ smaller than the amplitudes of the symmetric modes[21] (where r_{ij} is the intermetallic distance between the cations of a pair, $\lambda=vh/|J|$ is the wavelength of the resonant phonons, with v the sound velocity in the crystal), it would result that

$$\frac{A_{\text{pair}}}{A_{\text{single}}}\simeq\frac{1}{2}\alpha^2\frac{|J|^3}{\Delta^3}\ . \tag{18}$$

Here A_{pair} and A_{single} are the temperature-independent factors of the Orbach process rates, while $|J|$ and Δ are the splittings from the lowest levels involved in the ESR transitions, to the next higher level corresponding to the pairs and the single ions, respectively.[22]

By using the experimental values of $|J|=12.5$ K, $A_{\text{pair}}=(N_s/N_p)142.2=1.422\times10^4$, $\Delta=111.67$ K, $A_{\text{single}}=1.97\times10^8$, $v=3.136\times10^5$ m sec^{-1} and $r_{ij}=10^{-9}$ m, one obtains

$$\frac{A_{\text{pair}}}{A_{\text{single}}}=7\times10^{-5}$$

and

$$\tfrac{1}{2}\alpha^2\frac{|J|^3}{\Delta^3}\simeq5\times10^{-5}\ ,$$

respectively. Taking into account the approximations involved, these values are in good agreement with (18), supporting the assumption of an additional relaxation mechanism via paired Yb^{3+} ions.

Taking into consideration the above results one must reconsider the analysis of the experimental data obtained in the Q band.[8] This is done by subtracting the contribution from the pairs, which is magnetic-field independent and recalculating the temperature-independent factor of the direct process. Proceeding along these lines one can describe the overall low-temperature (2 K $\leq T\leq$ 12 K) relaxation data of the Yb^{3+} ions in SrF_2, in both X and Q frequency bands, for $g_{||}$, by the expression

$$T_1^{-1}=\frac{142.2}{\exp(12.5/T)-1}+7.731B^5\coth\frac{h\nu}{2kT}+0.197\times10^9\exp\left[-\frac{111.67}{T}\right], \tag{19}$$

where the magnetic field B is expressed in teslas.

At the lowest temperatures ($T\leq6$ K) only the first term in (19) is effective in the X band, while in the Q band, due to the strong magnetic-field dependence, the second term becomes dominant. For higher temperatures ($T\geq7.5$ K) the third term is dominant in both frequency bands.

The cross-relaxation at lower temperatures, between the single Yb^{3+} ions and pairs of exchange-coupled Yb^{3+} ions, can be used to explain the anomalous behavior of the shf structure of single Yb^{3+} ions. Indeed, by lowering the temperature, the shf structure due to the magnetic interaction of the single Yb^{3+} magnetic electrons with neighboring F^{19} nuclei is partly resolved, with an optimum around 11 K (Fig. 12). However, by doing measurements at lower temperatures (with microwave powers far below the saturating level) the shf structure becomes less resolved. At 4.2 K no resolved shf structure is visible any longer. This behavior is different from the one observed in the Q band.

In that case, once the shf is resolved (around 10 K), no changes take place by further lowering the temperature, even down to 1.4 K.

Such anomalous behavior, observed in the X band, can be explained if we notice that the "blurring" of the shf structure by going down in temperature takes place in the same temperature range where the cross-relaxation of single Yb^{3+} ions through Yb^{3+} pairs becomes effective. Consequently the linewidths of the individual shf transitions are determined by the cross-relaxation process, which is a fast one ($T_{21}=50$ μsec at 4.2 K). Consequently the individual shf transitions are lifetime broadened. Indeed, a similar relaxation time is obtained at higher temperatures, around 13.9 K where the shf structure is again unresolved.

The identification of exchange-coupled Yb^{3+} pairs in SrF_2 offers the opportunity to compare the characteristic parameters with similar ones, obtained from earlier studies. However, since our research, no such exchange-coupled pairs of rare-earth ions exhibiting overall trigonal symmetry have been yet reported.

Considering the simplest model of such a pair, as presented in Fig. 9, one can calculate the dipolar parameters in a point-dipole approximation. Since the intermetallic distance r is known (10^{-9} m), the dipolar contribution is calculated as

$$D_d^{\text{calc}}=-\frac{\beta^2}{3r_{ij}}(2g_{\parallel}^2+g_{\perp}^2)=-0.0043\ \text{cm}^{-1}\ .$$

The small value of D_d^{calc}, comparable to D_e (0.0089 cm^{-1}), confirms the model of weakly interacting magnetic ions in such a pair, in agreement with the proposed model.

Because we have not been able to determine the sign of D_e, there is an ambiguity in determining the exchange term D_E. If one takes both possible signs into account one still obtains values (-0.0046 cm^{-1} and $+0.0122$ cm^{-1}) of comparable magnitude, characteristic for weakly exchange-coupled pairs.

ACKNOWLEDGMENTS

The authors would like to thank Professor I. Ursu for valuable discussion and continuous support and Dr. A. A. Manenkov for kindly providing the samples used in this work.

[1]J. M. Baker in *Crystals with the Fluorite Structure,* edited by W. Hayes (Clarendon, Oxford, 1974), p. 341.

[2]U. Ranon and A. Yaniv, Phys. Lett. **9**, 17 (1964).

[3]S. V. Nistor, R. Baican, and C. Cernătescu, *Proceedings of the 18th Congress Ampère, Nottingham, 1974,* edited by P. S. Allen, E. R. Andrew, and C. A. Bates (Nottingham University Press, Nottingham, 1979), p. 149.

[4]A. A. Antipin, A. N. Katyshev, I. N. Kurkin, and L. A. Shekun, Fiz. Tverd. Tela (Leningrad) **9**, 3400 (1967) [Sov. Phys.—Solid State **12**, 2684 (1968)].

[5]R. C. Newman and R. J. Woodward, J. Phys. C **7**, L432 (1974).

[6]S. V. Nistor, R. Baican, and I. Ursu, *Proceedings of the 19th Congress Ampère, Heidelberg, 1976,* edited by H. Brunner, K. H. Hauser, and D. Schweitzer (Grupement Ampère, Heidelberg-Geneva, 1976), p. 173.

[7]B. G. Berulava, R. I. Mirianashvili, O. V. Nasarova, and T. S. Sanadze, Fiz. Tverd. Tela (Leningrad) **19**, 1771 (1977) [Sov. Phys.—Solid State **19**, 1033 (1977)].

[8]M. Velter-Stefănescu and S. V. Nistor, Phys. Status Solidi B **113**, K115 (1982).

[9]M. Velter-Stefănescu and B. Janculovici, Rev. Roum. Phys. **19**, 431 (1974).

[10]J. H. Van Vleck, Phys. Rev. **57**, 426 (1940).

[11]R. de L. Kronig, Physica **6**, 33 (1939).

[12]T. A. Giordmaine, L. E. Alsop, R. R. Nash, and C. H. Townes, Phys. Rev. **109**, 302 (1958).

[13]P. L. Scott and C. D. Jeffries, Phys. Rev. **127**, 32 (1962).

[14]K. J. Standley and R. A. Vaughan, *Electron Spin Relaxation Phenomena in Solids* (Hilger, London, 1969).

[15]M. Velter-Stefănescu and S. V. Nistor (unpublished).

[16]A. Löshe, in *Pulsed Magnetic and Optical Resonance,* edited by R. Blinc (Ljubljana, 1972), p. 131.

[17]I. Ursu, *La Resonance Paramagnetique Electronique* (Dunod, Paris, 1968).

[18]J. Owen and E. A. Harris, in *Electron Paramagnetic Resonance,* edited by S. Geshwind (Plenum, New York, 1972), p. 427.

[19]R. Orbach, Proc. R. Soc. London, Ser. A **264**, 458 (1961).

[20]J. C. Gill, Proc. Phys. Soc. London **79**, 58 (1962).

[21]A. M. Stoneham, Phys. Lett. **18**, 22 (1965).

[22]K. W. H. Stevens, Proc. R. Soc. London, Ser. A **214**, 237 (1952).